Conference materials
UDC 538.9
DOI: https://doi.org/10.18721/JPM.163.118

A change in the morphology of multilayer porous silicon with a stepwise decrease in the etching current density

A.S. Lenshin [1, 2], Ya.A. Peshkov [1] ✉, O.V. Chernousova [2], S.V. Kannykin [1],
M.V. Grechkina [1], D.A. Minakov [1], D.S. Zolotukhin [1], B.L. Agapov [1]

[1] Voronezh State University, Voronezh, Russia
[2] Voronezh State University of Engineering Technologies, Voronezh, Russia
✉ tangar77@mail.ru

Abstract. We present an experimental study of multilayer porous silicon formed by electrochemical etching. Special emphasis is placed on effects that arise from a stepwise decrease in the current density while maintaining the total etching time. In order to provide a fully understanding of the morphology of the surface, we used scanning electron and atomic force microscopy. X-ray reflectivity was used to assess the porosity of porous layers. It was found that a stepwise decrease in the current density leads to the formation of a two-layer structure without changing the porosity of the base bottom layer. However, the porosity of the top layer can be varied over a wide range, which directly affects the photoluminescence of the samples. Our results show how the sample production conditions affect the fine tuning of the surface layer morphology of multilayer porous silicon.

Keywords: porous silicon, multilayer nanostructures, X-ray reflectivity, surface morphology

Funding: This work was supported by the Russian Science Foundation Grant No. 19-72-10007. Part of the work was supported by a grant from the Ministry of Science and Higher Education of the Russian Federation No. FZGU-2020-0036.

Citation: Lenshin A.S., Peshkov Ya.A., Chernousova O.V., Kannykin S.V., Grechkina M.V., Minakov D.A., Zolotukhin D.S., Agapov B.L., A change in the morphology of multilayer porous silicon with a stepwise decrease in the etching current density, St. Petersburg State Polytechnical University Journal. Physics and Mathematics. 16 (3.1) (2023) 100–105. DOI: https://doi.org/10.18721/JPM.163.118

Материалы конференции
УДК 538.9
DOI: https://doi.org/10.18721/JPM.163.118

Изменение морфологии многослойного пористого кремния при ступенчатом уменьшении плотности тока травления

А.С. Леньшин [1,2], Я.А. Пешков [1] ✉, О.В. Черноусова [2], С.В. Канныкин [1],
М.В. Гречкина [1], Д.А. Минаков [1], Д.С. Золотухин [1], Б.Л. Агапов [1]

[1] Воронежский государственный университет, г. Воронеж, Россия
[2] Воронежский государственный университет инженерных технологий, г. Воронеж, Россия
✉ tangar77@mail.ru

Аннотация. Мы представляем экспериментальное исследование многослойного пористого кремния, полученного электрохимическим травлением. Особое внимание уделяется эффектам, возникающим в результате постепенного уменьшения плотности тока при сохранении общего времени травления. Было обнаружено, что, несмотря на режим травления, образуется двухслойная структура с различными показателями пористости. При этом, на фотолюминесценцию влияет только морфология верхнего слоя.

Ключевые слова: пористый кремний, многослойные наноструктуры, рентгеновская рефлектометрия, морфология поверхности

Финансирование: Работа выполнена при финансовой поддержке гранта РНФ № 19-72-10007. Часть работы была поддержана грантом Министерства науки и высшего образования Российской Федерации № FZGU-2020-0036.

Ссылка при цитировании: Леньшин А.С., Пешков Я.А., Черноусова О.В., Канныкин С.В., Гречкина М.В., Минаков Д.А., Золотухин Д.С., Агапов Б.Л. Изменение морфологии многослойного пористого кремния при ступенчатом уменьшении плотности тока травления // Научно-технические ведомости СПбГПУ. Физико-математические науки. 2023. Т. 16. № 3.1. С. 100–105. DOI: https://doi.org/10.18721/JPM.163.118

Introduction

Porous silicon (PSi) is a widely studied material that exhibits efficient visible photoluminescence at room temperature, a property not possessed by bulk silicon [1]. This unique feature allowed the PSi to expand quickly and flexibly for applications in nanophotonics, biosensors, and nanomedicine [2]. Recently, attempts have been made to form PSi as a buffer layer for the growth of thin films of various materials, from metals to III-V semiconductors [3]. The main advantage of PSi is the ability to control its surface morphology. Fine tuning of porosity, roughness, and pore size allows PSi to be used as a substrate that reduces mechanical stresses and improves adhesion. Moreover, the PSi buffer layer makes it possible to grow epitaxial thin films of materials with high lattice constant mismatch on silicon [4]. One type of adjustable porous substrate design is a multilayer nanostructure that has several alternating porous layers with different porosity (P) in each layer. It is possible to fabricate such multilayer PSi, since variations in the dielectric properties, and therefore the refractive index, can be easily obtained by changing the P or pore morphology, both of which are determined by the electrochemical anodization parameters. This paper presents the effect of production conditions on the surface morphology and photoluminescence of multilayer PSi.

Materials and Methods

The PSi samples were obtained by electrochemical etching (ECE) of single crystal silicon wafers. Multilayer PSi with different P values was obtained by varying the current density (J) of electrochemical anodization. The etching time (t) for all samples was the same (Table 1). The etching mode was chosen so that the average current density of the ECE was 35 mA/cm^2. X-ray reflectivity (XRR) was used to estimate the surface porosity value [5]. XRR is a non-destructive technique well used for the study of thin layers and multilayers. Unlike most other methods, it shows the dependence of the electron density on the depth of the sample under study. Since the critical angle for total reflection of X-rays from a layer is proportional to the mean density value of the layer, knowledge of the critical angle PSi ($\theta_{c\text{-}PS}$) and the crystalline silicon substrate ($\theta_{c\text{-}Si}$) allows us to calculate the porosity from the ratio: $P(\%)=[1-(\theta_{c\text{-}PS}/\theta_{c\text{-}Si})^2]\cdot 100$. XRR of PSi samples for porosity measurements was carried out using an ARL X'TRA X-ray diffractometer in the Bragg-Brentano geometry (Cu$K\alpha$). The surface morphology was studied by atomic force microscopy (AFM) and scanning electron microscopy (SEM). Image processing and data analysis were carried out with Gwyddion and ImageJ software [6, 7]. The photoluminescence (PL) spectra were recorded with an Ocean Optics USB4000-VIS-NIR fiber optic spectrometer; a laser diode with a radiation wavelength of 405 nm was used.

Results and Discussion

Figures 1, *a*, *b*, *c* show the results of SEM analysis performed on the cross-section of PSi layers obtained using different parameters of the etching current density of 35, 50/20 and 50/40/30/20 mA/cm^2, respectively. As can be seen from the SEM images, a two-layer structure

Table 1

PSi sample production conditions

Sample	Type and resistivity of the initial Si wafer, Ω×cm	J, mA/cm^2	t, min
1	n-type, phosphorus-doped, 0.2	35	4
2	n-type, phosphorus-doped, 0.2	50/20	2/2
3	n-type, phosphorus-doped, 0.2	50/40/30/20	1/1/1/1

is formed in multistep samples No. 2 and 3. The two PSi layers feature similar columnar-like morphology, with different thickness and porosity. It should be noted that an increase in the steps of changing the etching current density while maintaining the total etching time leads to a significant increase not only in the total thickness of the porous layer (L), but also in the thicknesses of the top (l_t) and bottom (l_b) layers (Table 2).

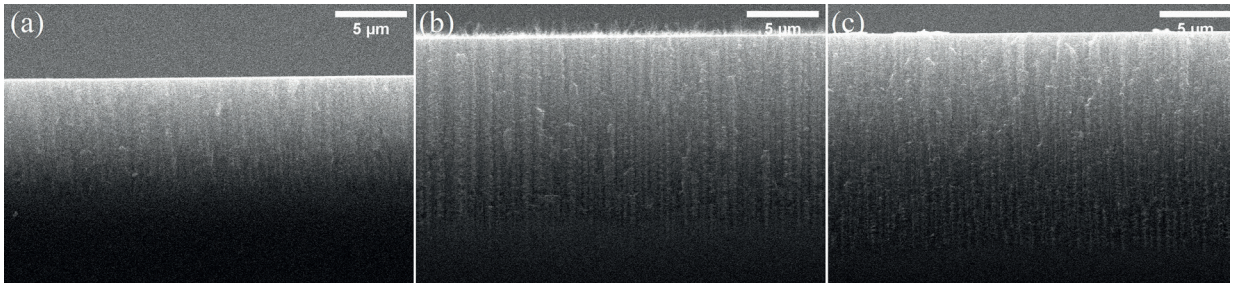

Fig. 1. Cross-section SEM images of PSi with a current density J of 35 mA/cm^2 (*a*), 50/20 mA/cm^2 (*b*) and 50/40/30/20 mA/cm^2 (*c*), respectively

Table 2

PSi morphology obtained from XRR measurements, SEM and AFM observations

Sample	P_t/P_b, %	z, nm	L, μm	l_t/l_b, μm
1	25/-	12	8.2	-
2	69/33	15	13.9	8.0/5.9
3	52/35	16	14.9	8.3/6.6

Figure 2 demonstrates the outcomes of atomic force microscopy (Fig. 2, *a*, *b*, *c*) performed on the samples surface obtained with different etching parameters. AFM analyses consistently show a mosaic-like surface with nanostructured silicon particles featuring peak-to-peak height (average value) of about 12–16 nm depending on the number of etch current density steps. In addition, the average size of silicon nanoparticles (z) increases from a single-stage sample to a four-stage one (Fig. 2, *d*). However, the root mean square roughness remains almost unchanged and is about 3 nm. The average pore diameter on the PSi surface was estimated from the analysis of SEM image data. All samples have approximately the same average pore diameter of about 200 nm.

Figure 3, *a* shows experimental XRR profiles taken from samples anodized under different conditions. From the critical angle, a coarse estimate of the average density of the top and bottom layers of a film can be calculated [8]. For reference, the XRR profile of a bulk *c*-Si crystal wafer is also shown ($\theta_{c\text{-}Si} \approx 0.22^\circ$ for $\lambda = 1.54$ Å) [5]. Single-stage sample No. 1 has one critical angle of total external reflection from the surface PSi layer with a porosity of about 25% which is consistent with the analysis of its cross-section SEM image. The experimental XRR profiles of two-layer samples reveal several features. For $\theta < \theta_{c\text{-}PS}$ there is a total reflection of the beam and all incoming X-rays are reflected from the surface ($\theta_{c\text{-}PS}$ is the critical angle of the PSi layer, which is smaller than $\theta_{c\text{-}Si}$ as the porous layer is less dense than *c*-Si). For θ values between the

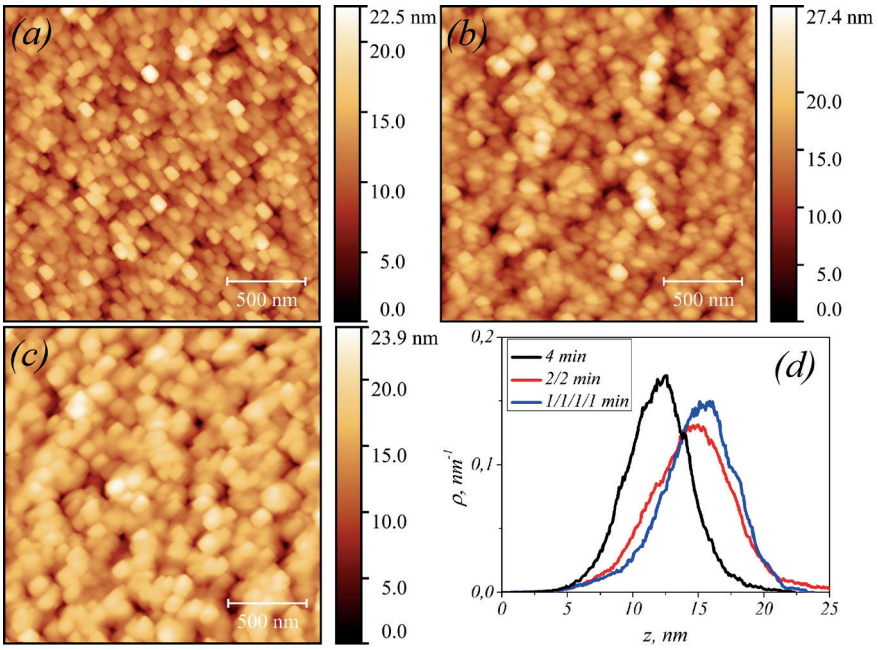

Fig. 2. AFM images of the PSi surface prepared at 35 (*a*), 50/20 (*b*), 50/40/30/20 mA/cm^2 (*c*), and silicon nanoparticles size distribution (*d*)

critical angles of the top and bottom PSi layers, the X-rays penetrate into the top porous layer but are totally reflected by the bottom porous layer. Thus, the reflected intensity is close to the incident one. For $\theta_{c\text{-}PS} < \theta$, X-rays penetrate both porous layers, leading to a strong decrease of the reflected intensity. XRR data for samples reveal that the porosity of the bottom base layer almost does not change (Table 2). The abrupt switching of the etching current density from 50 to 20 mA/cm^2 for a two-step sample led to the formation of a top PSi layer with a porosity of about 69%. A gradual decrease in the current density of the four-step sample formed a top layer with significantly lower porosity compared to sample No. 2.

Room temperature PL spectra from representative samples are shown in Fig. 3, *b*. The PL spectra exhibit a red shift as the porosity of the top porous layer increases, corresponding to the growth in average size of the crystalline Si domains in the sample. The PL spectrum of a single-stage sample with the lowest porosity of about 25% exhibits several features. In the region from 450 to 550 nm, a low-intensity peak appears corresponding to the luminescence of defects in the SiO_x oxide [9]. In addition, a more intense peak appears in the range from 550 to 800 nm.

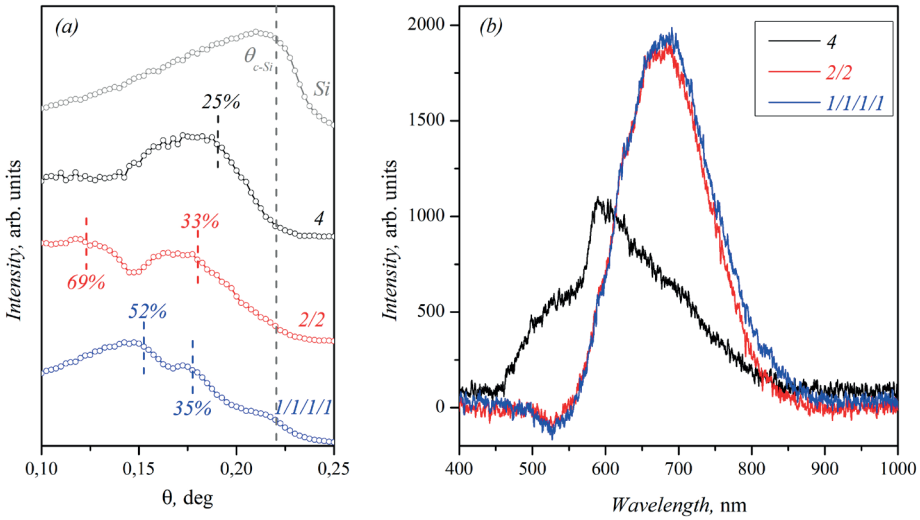

Fig. 3. XRR curves (*a*) of Si substrate and PSi produced under different production conditions and their PL spectra (*b*)

This effect is in good agreement with our previous study in which it was shown that in the porosity interval between 14 and 32% there is a transition to the quantum-size mechanism of the appearance of PL [10]. Multistage samples with highly porous top layers exhibit high-intensity PL in the 600 to 800 nm range. The position of the peak centered at 700 nm is usually associated with the luminescence of nanocrystals in PSi columns. According to theoretical and experimental data, silicon nanocrystals with a size of 2–3 nm luminesce in this range [1], although microscopy data shows a nanoparticle size of 12–16 nm. This can be explained by the fact that silicon column nanoparticles can simultaneously contain several silicon nanocrystals coated with an oxide shell.

Conclusion

We have fabricated a series of porous silicon multilayers with different layer thicknesses using electrochemical etching. An increase in the number of steps of changing the etching current density led to the formation of a two-layer structure with different porosity values. The average size of silicon nanoparticles, the pore diameter, and the surface roughness of all samples remain virtually unchanged. The total thickness of the porous silicon film increases with an increase in the number of steps of changing the current density. It is worth noting that changing the etching parameters affects the porosity of only the top layer while the porosity of the bottom layer remains almost unchanged. This leads to the fact that the position and intensity of the PL peak depends on the morphology and porosity of only the top layer, which is consistent with the penetration depth of the PL exciting radiation.

Acknowledgments

The research results were partially obtained with the scientific equipment of the Collective Use Center of Voronezh State University.

REFERENCES

1. **Canham L.,** Introductory lecture: origins and applications of efficient visible photoluminescence from silicon-based nanostructures, Faraday Discuss. 222 (2020) 10–81.

2. **Moretta R., De Stefano L., Terracciano M., Rea I.,** Porous silicon optical devices: recent advances in biosensing applications, Sensors. 21 (4) (2021) 1336.

3. **Seredin P.V., Len'shin A.S., Radam A.O., Khuder A.R., Goloshchapov D.L., Harajidi M.A., Arsentyev I.N., Kasatkin I.A.,** Properties of compliant substrates based on porous silicon formed by two-stage etching, Semiconductors. 56 (2022) 259–265.

4. **Sanchez-Perez C., Hernandez-Castro M., Garcia I.,** Engineering of ultra-thin sintered porous silicon virtual substrates for lattice-mismatched growth compliance and epilayer detachability, Appl. Surf. Sci. 577 (1) (2022) 151907.

5. **Daillant J., Gibaud A.,** X-ray and neutron reflectivity: principles and applications, Lect. Notes Phys. 770, Springer, Berlin Heidelberg, 2009.

6. **Nečas D., Klapetek P.,** Gwyddion: an open-source software for SPM data analysis, Open Physics. 10 (1) (2012) 181–188.

7. **Schneider C. A., Rasband W. S., Eliceiri K. W.,** NIH Image to ImageJ: 25 years of image analysis, Nat. Methods. 9 (2012) 671–675.

8. **Buttard D., Dolino G., Bellet D., Baumbach T., Rieutord F.,** X-ray reflectivity investigation of thin p-type porous silicon layers, Solid State Commun. 109 (1) (1998) 1–5.

9. **Zhang S.L., Huang F.M., Ho K.S., Jia L., Yang C.L., Li J.J., Zhu T., Chen Y., Cai S. M., Fujishima A., Liu Z.F.,** Two-peak photoluminescence and light-emitting mechanism of porous silicon, Phys. Rev. B. 51 (1995) 11194(R).

10. **Lenshin A.S., Peshkov Ya.A., Barkov K.A., Grechkina M.V., Lukin A.N., Kannykin S.V., Minakov D.A., Chernousova A.V.,** Features of the composition and photoluminescent properties of porous silicon depending on its porosity index, Coatings. 13 (2) (2023) 385.

THE AUTHORS

LENSHIN Alexander S.
lenshinas@phys.vsu.ru
ORCID: 0000-0002-1939-253X

PESHKOV Yaroslav A.
tangar77@mail.ru
ORCID: 0000-0003-0939-0466

CHERNOUSOVA Olga V.
byolval@mail.ru
ORCID: 0000-0002-8198-574X

KANNYKIN Sergey V.
svkannykin@gmail.com
ORCID: 0000-0001-8756-5722

GRECHKINA Margarita V.
grechkina_m@mail.ru
ORCID: 0000-0002-7873-8625

MINAKOV Dmitriy A.
lenshinas@mail.ru
ORCID: 0000-0002-3956-196X

ZOLOTUKHIN Dmitriy S.
zolotuhin@phys.vsu.ru
ORCID: 0000-0002-9645-9363

AGAPOV Boris L.
b.agapov2010@yandex.ru

Received 10.07.2023. Approved after reviewing 10.08.2023. Accepted 10.08.2023.